Article:
Romanova, T, Stoyan, Y, Pankratov, A et al. (6 more authors) (2021) Optimal layout of ellipses and its application for additive manufacturing. International Journal of Production Research, 59 (2). pp. 560-575. ISSN 0020-7543

https://doi.org/10.1080/00207543.2019.1697836

Optimal layout of ellipses and its application for Additive Manufacturing

Romanova, Tatiana[*1a], Stoyan, Yuri[1a], Pankratov, Alexandr[1a], Litvinchev, Igor[2], Avramov, Konstantin[1b], Chernobryvko, Marina[1b], Yanchevskyi, Igor[3], Mozgova, Irina[4], Bennell, Julia[5]

[1]*Institute for Mechanical Engineering Problems of the National Academy of Sciences of Ukraine,* [a]*Department of Mathematical Modelling and Optimal Design,* [b]*Department of Reliability and Dynamic Strength, Kharkiv, Ukraine*
[2]*Nuevo Leon State University (UANL), Faculty of Mechanical and Electrical Engineering, San Nicolas de los Garza, Mexico*
[3]*National Technical University of Ukraine "Igor Sikorsky Kyiv Polytechnic Institute", Department of Dynamics and Strength of Machines and Strength of Materials, Kyiv, Ukraine*
[4]*Institute of Product Development, Leibniz University of Hannover, Hannover, Germany*
[5]*Leeds University Business School, University of Leeds, Leeds, UK*

The paper studies a layout problem of variable number of ellipses with variable sizes placed into an arbitrary disconnected polygonal domain with maximum packing factor. The ellipses can be continuously translated and rotated. Restrictions on the dimensions of the ellipses are taken into account. Tools for the mathematical modeling of placement constraints (distance constraints between ellipses and containment of ellipses into a polygonal domain) using the phi-function technique are introduced. The tools make it possible to formulate the layout problem in the form of MIP model that is equivalent to a sequence of nonlinear programming subproblems. We develop a new solution algorithm that involves the feasible starting point algorithm and optimization procedure to search for efficient locally optimal solutions of the layout problem. This algorithm can be used in the design of parts for «support-free» additive manufacturing, taking into account the conditions for its static/ dynamic strength. Results of the algorithm implementation for a topologically optimized flat part with the analysis of a stress state are provided.

Keywords: ellipses; layout; phi-function technique; mathematical model; nonlinear optimization; additive manufacturing

1. Introduction

The layout problem presented in this work is motivated by designing parts (3D objects) with complex geometry for their production using additive manufacturing (AM) technology (Gibson, Rosen, and Stucker 2015; Liu and Ma 2016; Araújo Luiz et al. 2018), also known as 3D printing. AM is the process of creating parts as opposed to traditional subtractive manufacturing methods. AM is an appropriate name to describe the technologies that build 3D objects by adding layer-upon-layer of material. In (Araújo Luiz et al. 2018) a review of existing general cutting and packing taxonomies in AM is presented and new specifications for classifying the problems encountered in AM are discussed. In particular, the build volume packing task in AM is formulated as a three-dimensional irregular problem of packing nonconvex polyhedra in an optimized cuboid container (see, e.g., (Romanova et al. 2018)).

In this paper we consider another application of packing problems in AM. The popular AM approach implies inserting in the part geometry so-called “supports” at the pre-manufacturing/production

[*] _Corresponding author. Email: tarom27@yahoo.com

stage (Leary et al. 2016). The supports then have to be removed thus increasing duration and cost of production. The "support-free" technologies are free from this disadvantage. In (Gibson, Rosen, and Stucker

2015) based on identified design for additive manufacture rules, a method is proposed that modifies the theoretically optimal topology as required to ensure manufacturability without requiring additional support material.

Paper (Mokwon et al. 2018) presents a novel method for generating support-free elliptic hollowing for 3D shapes avoiding additional supporting structures. To pack ellipses in the polygon the Voronoi diagram is used. In this paper novel mathematical techniques for preparing part geometry for "support-free" production are presented. The main idea is replacing material-free part volumes not suitable for AM technologies (see, e.g., (Leary et al. 2016)) by an elliptical cavity system.

The parameters of our algorithm are the minimum allowed distance between ellipses and restrictions on their sizes. In contrast to (Gibson, Rosen, and Stucker 2015), our design is less sensitive to orientation of the part during its additive production. The part produced with elliptical cavities is also more durable due to the absence of sharp internal corners (stress concentrators). The parts with simple geometric shape cavities are more suitable for subsequent "finishing" technological operations. It is important for improving the quality of the part surfaces to increase their fatigue strength and durability, while making it more visually aesthetics (Huang and Xie 2010). The approach can be naturally combined with existing optimal design algorithms focused on ensuring the part strength while minimizing its weight (see, e.g., (Liu and Tovar 2014)). This may lead to creating a system of automated part design for direct "support-free" production with the ability to predict even at the design stage their static/dynamic/fatigue strength depending on the type of operational loads. The optimal layout for ellipses in a system of disconnected polygonal regions, considered in the paper, is closely connected with the problem of minimizing the mass of the finished part. Special technical requirements (Lachmayer and Lippert 2017), e.g. minimum wall thickness, minimum/maximum radius of curvature of the internal surfaces can also be taking into account.

In this work a case study of implementing our algorithm for preparing a part for additive manufacturing is presented. The initial geometry of the part is obtained by topological optimization. The result of the design is compared with alternative geometries for maximum mechanical stresses under the action of a static cantilever load. These calculations are performed using the finite element method using a specialized software package.

From mathematical point of view, this paper considers a new problem of optimal layout ellipses in a disconnected polygonal region with convex components of connectedness. This problem arises in computational geometry and operational research (Leao Aline et al. 2019; Fasano 2015). In recent years the problem of optimal placement for ellipses was intensively studied by different authors (see, e.g., (Litvinchev, Infante, and Ozuna 2015a; Pankratov, Romanova, and Litvinchev 2018; Stoyan, Pankratov, and Romanova 2016; Kampas, Castillo, and Pintér 2019; Emmendorfer, Oro, and Beckel 2015; Kallrath

and Rebennack 2014; Birgin, Lobato, and Martinez 2016; Pankratov, Romanova, and Litvinchev 2019) and the references therein).

In (Litvinchev, Infante, and Ozuna 2015a) a problem of packing different circular objects in a rectangular container is considered maximizing the total number of objects placed into the container. Varying the norm used in the definition of the circular object different shapes can be obtained, including ellipses. Using a grid approximation of the container the packing problem is stated as a large scale linear 0-1 optimization problem with binary variables representing assignment of centers to the nodes of the grid. Valid inequalities are used to strengthening the original formulation. Modifications of the main model are proposed to take into account nesting and/or thickness of the circles. The paper (Pankratov, Romanova, and Litvinchev 2018) studies packing ellipses in a rectangular container of minimum area. New tools are proposed for non-overlapping and containment constraints. A mathematical model for the packing problem is stated as a nonlinear programming problem. Two algorithms to find feasible starting points for identical and non-identical ellipses are proposed. The optimization procedure is used as a compaction algorithm to search for local optimal solutions. Paper (Stoyan, Pankratov, and Romanova 2016) introduces quasi-*phi*-functions for an analytical description of placement constraints for free rotated and translated objects. For the packing ellipses into a minimum-area rectangle a mathematical model is formulated using quasi-*phi*-functions. The nonlinear programming problem is solved by an efficient solution technique proposed in the paper. In (Kampas, Castillo, and Pintér 2019) the authors present a model and numerical solution approach for packing ellipses into an optimized regular polygon. The optimization strategy is based on the concept of embedded Lagrange multipliers. They proceed simultaneously towards these objectives using the "LGO" solver system for global-local nonlinear optimization. The paper (Emmendorfer, Oro, and Beckel 2015) presents a heuristic developed for packing problems of a number of non-identical ellipses of variable sizes into an irregular polygon. Packed ellipses are tangent to the master ellipse, initially positioned at the center of the polygon. Superposition restrictions are imposed and checked at each stage. In (Kallrath and Rebennack 2014) the packing ellipses in a rectangle of minimum area is considered. The ellipses allow free rotations. A mathematical programming formulation for this problem is presented. For more than 14 ellipses the paper proposes heuristics. In (Birgin, Lobato, and Martinez 2016) continuous nonlinear programming models and algorithms for packing n-dimensional ellipsoids in a minimum-area container are introduced. Two different models for the non-overlapping and models for the inclusion of ellipsoids within half-spaces and ellipsoids are presented. The authors apply a multi-start strategy combined with a clever choice of starting guesses and nonlinear programming local solver. Paper (Pankratov, Romanova, and Litvinchev 2019) considers packing ellipses with arbitrary orientation into a convex polygon. The objective is to find a minimum homothetic coefficient for the polygon still containing a given collection of ellipses. New phi-functions and quasi phi-functions to describe placement constraints are introduced. The packing problem is stated as a nonlinear programming problem. A solution approach is proposed combining a new starting point algorithm and a new algorithm to search for locally

optimal solutions.

Paper contributions:

1. New statement of the ellipse packing problem that has application in AM for the topological optimisation of final products.
2. New tools for the mathematical modelling of distance and containment constraints for a *variable number* of *variable-size* free rotated ellipses packed into a *disconnected polygonal domain*.
3. Novel *mathematical models* of the ellipse packing problem.
4. New algorithm for constructing *starting feasible points* for the ellipse packing problem.
5. New local optimisation procedure that *reduces* the ellipse packing problem *dimension*.

This paper is organized as follows. In Section 2 we give a new statement of the layout problem of ellipses in a disconnected polygonal domain. Section 3 describes new tools for the mathematical modeling of distance and containment constraints for a variable number of variable-size free rotated and translated ellipses packed into a disconnected polygonal domain. Section 4 gives new mathematical models of the problem. A novel algorithm for constructing feasible starting points and new optimization procedure to reduce the computational cost of the ellipse packing problem are presented in section 5. In Section 6 we demonstrate the efficiency of the proposed algorithm.

2. Problem statement

We describe a polygonal domain by the union of a finite number of disjoint convex polygons: $\Omega=\bigcap_{q=1}^{N}\mathbf{P}_q,\ \mathbf{P}_{q_1}\cap\mathbf{P}_{q_2}=\varnothing,\ q_1,q_2\in I_N=\{1,\ldots,N\},q_1<q_2,$ where $\mathbf{P}_q$ is a convex polygon.

Let us consider a family $\mathbf{E}$ of ellipses with variable semi-axes $a\le a',\ b\ge b',\ a\ge b,\ d'\le\frac{a}{b}\le d'',$ where a',b',d',d'' are the given constants, i.e. $\mathbf{E}=\{E\,|\,a\ge b,a\le a',b\ge b',d'\le\frac{a}{b}\le d''\}$.

Our aim is to generate the N ellipse subsets $\mathbf{E}^q=\left\{E_i^q\in\mathbf{E},i\in J^q\right\},\ q\in I_N,\ J^q=\{1,\ldots,n_q\},$ that can be fully arranged without overlapping inside the appropriate convex polygons $\mathbf{P}_q,\ q\in I_N,$ with the maximum packing factor.

In addition, a minimum allowable distance $\rho>0$ between each pair of the ellipses E_i^q and E_j^q is given for $i,j\in J^q,\ i<j.$

A subset $\mathbf{E}^q$ of variable-size moving ellipses is denoted by $\mathbf{E}^q(u^q)=\{E_i^q(u_i^q),i\in J^q\}$, where $u^q=(u_1^q,u_2^q,\ldots,u_{n_q}^q)\in\mathbf{R}^{5n_q}$ is a vector of variable parameters of the ellipses $E_i^q(u_i^q),\ i\in J^q,$

$u_i^q=(x_i^q,y_i^q,\theta_i^q,a_i^q,b_i^q)$, $v_i^q=(x_i^q,y_i^q)$ is a translation vector; θ_i^q is a rotation angle; a_i^q,b_i^q are semi-axes of the ellipse E_i^q.

Ellipse Layout Problem in a Disconnected Polygonal Domain (ELD). Find such ellipse subsets $\mathbf{E}^q(u^{q*})$, $u^{q*}=(u_1^{q*},u_2^{q*},\ldots,u_{n^q}^{q*})$, $q\in I_N$, that can be fully arranged within the appropriate convex polygons $\mathbf{P}_q$, $q\in I_N$, with the maximum occupied area $F_q^*(u^{q*})=\pi\sum_{i=1}^{n_q*}a_i^{q*}b_i^{q*}$, taking into account the given minimum allowable distance ρ between the ellipses.

A value $F^*(u^*)=\sum_{q=1}^{N}F_q^*(u^{q*})$ is taken as a solution of the problem of the maximum filling of the whole disconnected domain Ω, where $u^*=(u^{1*},u^{2*},\ldots,u^{N*})$.

The problem is equvalent to a sequence of N independent layout subproblems for each $q\in I_N$ in the following formulation.

Ellipse Layout Problem in a Convex Polygon (ELC). Find u^{q*} and n_q^* such that the ellipses $E_i^q(u_i^{q*})\in\mathbf{E}^q$, $i\in I_{n_q^*}$, are packed in a convex polygon $\mathbf{P}_q$, taking into account distance constraints, such that the packing factor will reach its maximum value.

In ELC problem the following layout constraints are met:

- Containment constraints: $E_i^q(u_i^q)\subset\mathbf{P}_q$ for each $i\in I_{n_q}$;
- Distance constraints for the ellipses $E_i^q(u_i^q)$ and $E_j^q(u_j^q)$ for each $i<j\in I_{n_q}$:

$$\mathrm{dist}(E_i^q(u_i^q),\ E_j^q(u_j^q))\geq\rho,$$

where $\rho>0$, $\mathrm{dist}(E_i^q,E_j^q)=\min\limits_{e_i\in E_i^q,e_j\in E_j^q}\mathrm{d}(e_i,e_j)$, $\mathrm{d}(e_i,e_j)$ is the Euclidean distance between the two points e_i,e_j.

In this study, we use the *phi*-function technique (Stoyan et al. 2015; Stoyan, Pankratov, and Romanova 2015; Stoyan and Romanova 2013; Chernov, Stoyan, and Romanova 2010) as the powerful tool of mathematical modeling of the layout constraints.

3. Mathematical modelling tools

In this section we introduce a *phi*-function to describe containment constraint $E_i^q(u_i^q) \subset \Omega$ and normalized quasi *phi*-function to describe distance constraint dist($E_i^q(u_i^q)$, $E_j^q(u_j^q)$) $\geq \rho$.

For the *phi*-function and quasi-*phi*-function definitions we refer the reader to (Stoyan, Pankratov, and Romanova 2016; Chernov, Stoyan, and Romanova 2010).

In order to define our functions for the sake of simplicity we omit the index q for ellipses.

3.1 *Phi-function for containment constraints*

Containment of the ellipse $E_i(u_i)$ into Ω for ELD

Let $\Omega = \bigcup_{q=1}^{N} \mathbf{P}_q$, $\mathbf{P}_{q_1} \cap \mathbf{P}_{q_2} = \varnothing, \mathbf{P}_{q_1} \cap \mathbf{P}_{q_2} = \varnothing$, $q_1, q_2 \in I_N = \{1,\ldots,N\}$, $q_1 < q_2$, where $\mathbf{P}_q$ is a convex polygon.

We define the *phi*-function of $E_i(u_i)$ and object $\Omega^* = R^2 \setminus \text{int}\Omega$ in the form

$$\Phi^{E_i\Omega^*}(u_i) = \max_{q \in I_N} \Phi^{E_i\mathbf{P}_q^*}(u_i), \tag{1}$$

where $u_i = (x_i, y_i, \theta_i, a_i, b_i)$, $\Phi^{E_i\mathbf{P}_q^*}(u_i)$ is the *phi*-function of $E_i(u_i)$ and the object $\mathbf{P}_q^* = R^2 \setminus \text{int}\mathbf{P}_q$ (Fig. 1) defined in the next Subsection.

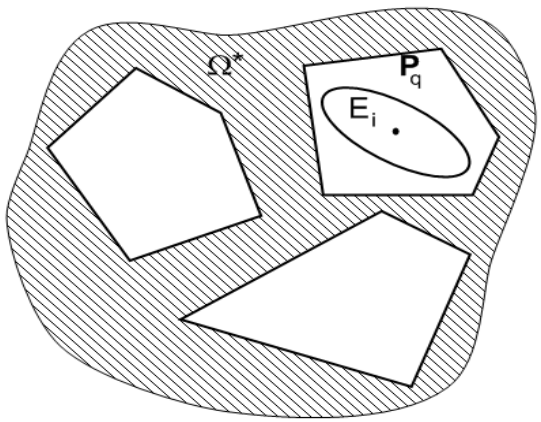

Fig. 1 – Ellipse $E_i(u_i)$ and object Ω^*

Containment of the ellipse $E_i(u_i)$ into $\mathbf{P}_q$ for ELC

Let $\mathbf{P}_q$ be a convex polygon given in the form $\mathbf{P}_q = \bigcap_{s=1}^{m_q} P_{qs}$, where $P_{qs} = \{(x,y)$: $\mu_s^q = x \cdot \cos\phi_{qs} + y \cdot \sin\phi_{qs} + \gamma_{qs} \geq 0\}$ is a half plane; $\phi_{qs} = \text{const}$; $\gamma_{qs} = \text{const}$; $L_{qs} = \{(x,y): \mu_s^q = 0\}$;

$\mu_s^q = 0$ is the normal equation of the s-th side of $\mathbf{P}_q$ ($s \in I_{m_q}$).

The *phi*-function of the ellipse $E_i(u_i)$ from the family $\mathbf{E}$ and the object $\mathbf{P}_q^*$ can be defined in the form

$$\Phi^{E_i \mathbf{P}_q^*}(u_i) = \min\{\Phi_{is}^{q*}(u_i), s \in I_m\}, \tag{2}$$

where

$$\Phi_{is}^{q*}(u_i) = \delta_{is}^q(x_i, y_i) - d_{is}^q(\theta_i, a_i, b_i) \tag{3}$$

is the *phi*-function of the ellipse $E_i(u_i)$ and half plane $P_{qs}^* = R^2 \setminus \mathrm{int} P_{qs}$,

$$u_i = (x_i, y_i, \theta_i, a_i, b_i),\ d_{is}^q(\theta_i, a_i, b_i) = \sqrt{a_i^2 \cdot \cos^2(\theta_i + \phi_{qs}) + b_i^2 \cdot \sin^2(\theta_i + \phi_{qs})},$$

$$\delta_{is}^q(x_i, y_i) = x_i \cos\phi_{qs} + y_i \sin\phi_{qs} + \gamma_{qs}.$$

The inequality $\Phi_{is}^{q*}(u_i) \geq 0$ provides the non-overlapping of $E_i(u_i)$ and P_{qs}.

Therefore, according to (2), the inequality $\Phi^{E_i \mathbf{P}_q^*}(u_i) \geq 0$ implies the containment constraint $E_i(u_i) \subset \mathbf{P}_q$, i.e. $\mathrm{int} E_i(u_i) \bigcap \mathrm{int} \mathbf{P}_q^* = \varnothing$.

3.2 *Normalized quasi phi-function for distance constraints*

Let us construct a normalized quasi-*phi*-function for the ellipses $E_i(u_i)$ and $E_j(u_j)$ with variable placement parameters (x_i, y_i, θ_i), (x_j, y_j, θ_j) and variable sizes (a_i, b_i), (a_j, b_j) that describes analytically the distance constraint $\mathrm{dist}(E_i(u_i), E_j(u_j)) \geq \rho$.

The key idea is based on the following statement. Let $L_{ij} = \{(x, y) \in R^2 : \cos\phi_{ij} x + \sin\phi_{ij} y = 0\}$ be a straight line, passing through the coordinate system origin *O*, where ϕ_{ij} is an angle between the straight line L_{ij} and axis $O X$.

We assume that the distance between two ellipses E_i and E_j is equal to ρ under some parameters u_i and u_j. It means that there is always exists an angle ϕ_{ij}^* such that the distance between the projections of the ellipses on this line, denoted by e_{ij}^* and e_{ji}^*, is equal to ρ (Fig. 2a). We note that the distance ρ' between e_{ij} and e_{ji} is less than or equal to ρ for the other values of variable ϕ_{ij} (Fig. 2b).

A normalized quasi-*phi*-function $\Phi'^{E_iE_j}(u_i,u_j,\phi_{ij})$ of the ellipses $E_i(u_i)$ and $E_j(u_j)$ from the family **E** can be defined in the form

$$\Phi'^{E_iE_j}(u_i,u_j,\phi_{ij}) = f_{ij}(v_i,\phi_{ij}) - f_{ji}(v_j,\phi_{ij}) - g_{ij}(\theta_i,\phi_{ij},a_i,b_i) - g_{ji}(\theta_j,\phi_{ij},a_j,b_j), \qquad (4)$$

where $\phi_{ij} \in R^1$, $u_i = (x_i, y_i, \theta_i, a_i, b_i)$, $u_j = (x_j, y_j, \theta_j, a_j, b_j)$,

$$f_{ij}(v_i,\phi_{ij}) = x_i\cos\phi_{ij} - y_i\sin\phi_{ij},\ f_{ji}(v_j,\phi_{ij}) = x_j\cos\phi_{ij} - y_j\sin\phi_{ij},$$

$$g_{ij}(\theta_i,\phi_{ij},a_i,b_i) = \sqrt{a_i^2\cos^2(\theta_i-\phi_{ij}) + b_i^2\sin^2(\theta_i-\phi_{ij})},$$

$$g_{ji}(\theta_j,\phi_{ij},a_j,b_j) = \sqrt{a_j^2\cos^2(\theta_j-\phi_{ij}) + b_j^2\sin^2(\theta_j-\phi_{ij})}.$$

The quasi-*phi*-function (4) is a normalized one, because $\max_{\phi_{ij}} \Phi'^{E_iE_j}(u_i,u_j,\phi_{ij})$ is the normalized *phi*-function of the ellipses $E_i(u_i)$ and $E_j(u_j)$.

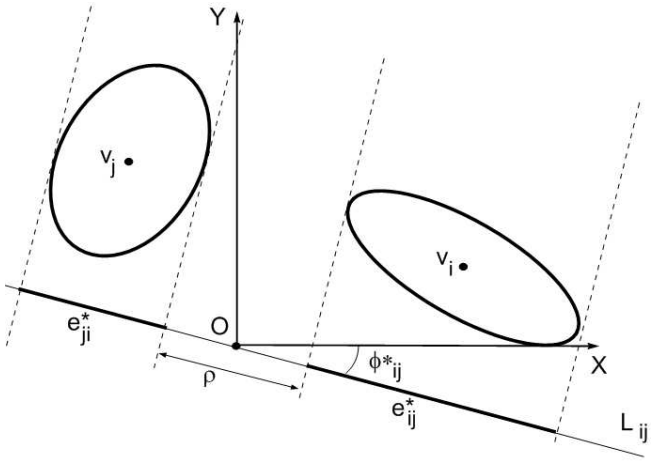

a

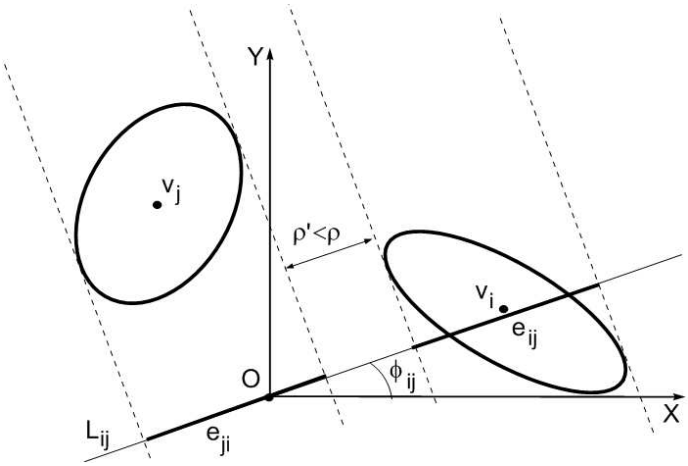

b

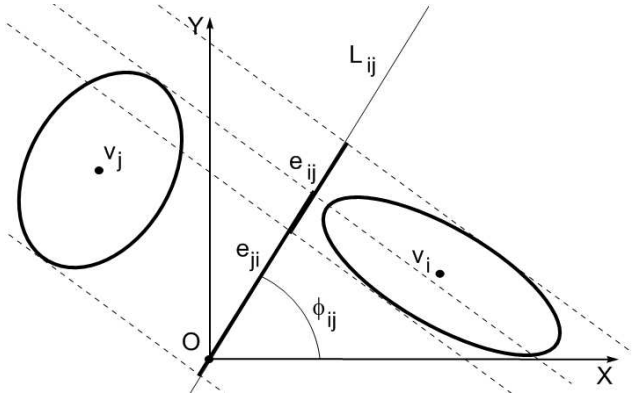

c

Fig. 2 – Illustration to the normalized quasi-*phi*-function $\Phi'^{E_iE_j}$. The distance between ellipses E_i and E_j is equal to $\rho>0$ and the distance between their projections e_{ij} and e_{ij} is equal to ρ': a) $\rho'=\rho$, $\Phi'^{E_iE_j}=\rho$; b) $\rho'<\rho$, $\Phi'^{E_iE_j}=\rho'$; c) $\rho'=0$, $\mathrm{int}e_{ij}\bigcap\mathrm{int}e_{ji}\neq\varnothing$, $\Phi'^{E_iE_j}<0$

Thus $\max\limits_{\phi_{ij}}\Phi'^{E_iE_j}(u_i,u_j,\phi_{ij})=\Phi'^{E_iE_j}(u_i,u_j,\phi_{ij}^*)=\rho$.

We note that if $\mathrm{int}E_i(u_i)\bigcap\mathrm{int}E_j(u_j)\neq\varnothing$ values of the normalized quasi-*phi*-function $\Phi'^{E_iE_j}(u_i,u_j,\phi_{ij})$ for any ϕ_{ij} are negative (Fig.2c).

Besides, the quasi-*phi*-function (4) is considerably simpler than the quasi-*phi*-function for the two ellipses considered in (Stoyan, Pankratov, and Romanova 2016). It contains one auxiliary variable (in construct to four variables in (Stoyan, Pankratov, and Romanova 2016)) and just one function (in construct to six functions in (Stoyan, Pankratov, and Romanova 2016)).

Thus, based on the features of the normalized quasi-*phi*-function (Stoyan, Pankratov, and Romanova 2016) we can conclude that $\Phi'^{E_iE_j}(u_i,u_j,\phi_{ij})\geq\rho$ implies $\mathrm{dist}(E_i(u_i),E_j(u_j))\geq\rho$.

4. Mathematical model

4.1 *Model of ELD*

Let us consider a collection of ellipses E_i $(i\in I_n)$, from the family $\mathbf{E}$, where $n=\sum\limits_{q=1}^{N}\left\lceil\frac{S_q}{\pi b'^2}\right\rceil$, S_q is the area of $\mathbf{P}_q\subset\Omega$.

The ELD problem can be formulated in the form of the following Mixed Integer Problem (MIP):

$$(z^*,u^*,\phi^*)=\arg\max_{(z,u,\phi)\in W\subset R^\sigma} F(z,u,\phi), \tag{5}$$

$$W=\{(z,u,\phi)\in R^\sigma : z_i\cdot z_j\cdot\Phi'^{E_iE_j}(u_i,u_j,\phi_{ij})-z_i\cdot z_j\cdot\rho\geq 0, i<j\in I_n, \tag{6}$$

$$z_i\cdot\Phi^{E_i\Omega^*}(u_i)\geq 0, a_i\geq b_i, b_i\geq b', a_i\leq a', d'\leq\frac{a_i}{b_i}\leq d'', i\in I_n\},$$

where

$$F(z,u,\phi)=\pi\sum_{i=1}^{n} z_i\cdot a_i\cdot b_i,\ z=(z_1,\ldots,z_n),\ z_i\in\{0,1\},$$

$$u=(u_1,u_2,\ldots,u_n),\ u_i=(x_i,y_i,\theta_i,a_i,b_i);\ \phi=(\phi_{12},\phi_{13},\ldots,\phi_{n,n-1});\ \sigma=6n+\frac{n(n-1)}{2},$$

$\Phi'^{E_iE_j}(u_i,u_j,\phi_{ij})$ is the normalized *phi*-function for the ellipses $E_i(u_i)$ and $E_j(u_j)$ defined in (4); $\Phi^{E_i\Omega^*}(u_i)$ is the *phi*-function for the ellipse $E_i(u_i)$ and object Ω^* defined in (1). Note that in (5)-(6) z,u,ϕ are variables to optimize. Here binary variables are defined as follows: $z_i=1$ if the ellipse $E_i(u_i)$ belongs to Ω and $z_i=0$ otherwise.

This model can be applied for the layout of variable radius circles. In this particular case we set $a_i=b_i=r_i$ and replace: the quasi-*phi*-function $\Phi'^{E_iE_j}(u_i,u_j,\phi_{ij})$ by the normalized *phi*-function $\Phi'^{C_iC_j}(x_i,y_i,r_i,x_j,y_j,r_j)$ for two circles $C_i(x_i,y_i,r_i)$ and $C_j(x_j,y_j,r_j)$; the *phi*-function $\Phi^{E_i\Omega^*}(u_i)$ by the *phi*-function $\Phi^{C_i\Omega^*}(x_i,y_i,r_i)$ for the circle $C_i(x_i,y_i,r_i)$ and the object Ω^*. The number of variables of the circular layout problem is $\sigma=3n$.

By (1) the problem (5)-(6) is equivalent to N independent subproblems of layout ellipses in a convex polygon $\mathbf{P}_q$ ($q\in I_N$) (ELC problem). We describe the q-th subproblem in Subsection 4.2.

4.2 *Mixed Integer Model of ELC*

Now we consider a collection of the ellipses $E_i^q, i\in I_{n_q}$, of dimensions a_i^q and $b_i^q, i\in I_{n_q}$, where $n_q=\left\lceil\frac{S_q}{\pi b'^2}\right\rceil$, S_q is the area of $\mathbf{P}_q$.

The ELC problem can be formulated in the form of the following Mixed Integer Problem (MIP):

$$(z^{q*},u^{q*},\phi^{q*})=\arg\max_{(z^q,u^q,\phi^q)\in W_q\subset R^{\sigma_q}} F_q(z^q,u^q,\phi^q), \tag{7}$$

$$W_q = \{(z^q, u^q, \phi^q) \in R^{\sigma_q} : z_i^q \cdot z_j^q \cdot (\Phi'^{E_i^q E_j^q}(u_i^q, u_j^q, \phi_{ij}^q) - \rho) \geq 0, i < j \in I_{n_q}, \tag{8}$$

$$g_i^q \cdot \Phi^{E_i^q \mathbf{P}_q^*}(u_i^q) \geq 0, a_i^q \geq b_i^q, b_i^q \geq b', a_i^q \leq a', d' \leq \frac{a_i^q}{b_i^q} \leq d'', i \in I_{n_q}\},$$

where

$$F_q(z^q, u^q, \phi^q) = \pi \sum_{i=1}^{n_q} z_i^q \cdot a_i^q \cdot b_i^q,$$

$$z^q = (z_1^q, \ldots, z_{n_q}^q),\ u^q = (u_1^q, u_2^q, \ldots, u_{n_q}^q),\ u_i^q = (x_i^q, y_i^q, \theta_i^q, a_i^q, b_i^q),\ \phi^q = (\phi_{12}^q, \phi_{13}^q, \ldots, \phi_{n_q, n_q-1}^q),$$

$$\sigma_q = 6n_q + \frac{n_q(n_q-1)}{2},\ z_i^q \in \{0,1\}.$$

$\Phi'^{E_i^q E_j^q}$ is the normalized quasi-*phi*-function for the ellipses $E_i(u_i^q)$ and $E_i^q(u_j^q)$ defined in (4); $\Phi^{E_i^q \mathbf{P}_q^*}$ is the *phi*-function for the ellipse $E_i^q(u_i^q)$ and object $\mathbf{P}_q^*$ defined in (2). Here binary variables are defined as follows: $z_i^q = 1$ if the ellipse $E_i(u_i)$ belongs to $\mathbf{P}_q$ and $z_i^q = 0$ otherwise.

The MIP model (7)-(8) is equivalent to n_q independent nonlinear programming (NLP) subproblems of packing $t = 1,2,\ldots,n_q$ ellipses. Each subproblem (called **ELP**) searches for the placement parameters and sizes of the maximum total area t ellipses within a convex polygon $\mathbf{P}_q$.

4.3 *Nonlinear Continuous Model of ELP*

Now we assume that $E_i^q \in \mathbf{E}^q$ $(i \in I_t)$, and introduce the following NLP subproblem:

$$(u^{q*}, \phi^{q*}) = \arg \max_{(u^q, \phi^q) \in W_q \subset R^\sigma} F_q(u^q, \phi^q), \tag{9}$$

$$W_q = \{(u^q, \phi^q) \in R^\sigma : \Phi'^{E_i^q E_j^q}(u_i^q, u_j^q, \phi_{ij}^q) \geq \rho, (i,j) \in \Xi, \tag{10}$$

$$\Phi^{E_i^q \mathbf{P}_q^*}(u_i^q) \geq 0, a_i^q \geq b_i^q, b_i^q \geq b', a_i^q \leq a', d' \leq \frac{a_i^q}{b_i^q} \leq d'', i \in I_t\},$$

where

$$F_q(u^q, \phi^q) = \pi \sum_{i=1}^{t} a_i^q b_i^q,\ u^q = (u_1^q, \ldots, u_t^q),\ \phi^q = (\phi_{12}^q, \ldots, \phi_{t-1,t}^q),\ u_i^q = (x_i^q, y_i^q, \theta_i^q, a_i^q, b_i^q),$$

$$\sigma = 5t + \frac{t(t-1)}{2},\ \Xi = \{(i,j) : i < j \in I_t\},$$

$\Phi'^{E_i^q E_j^q}(u_i^q, u_j^q, \phi_{ij}^q)$ is defined in (4); $\Phi^{E_i^q \mathbf{P}_q^*}(u_i^q)$ is defined in (2).

We denote the local optimal point found for the problem (9)-(10) by (u^{q*}, ϕ^{q*}).

5. Solution algorithm

5.1 *Algorithm for ELD*

Our algorithm solves problem (5)-(6) and can be described by the following steps:

Step 1. Set $q=1$.

Step 2. Set $t=1$, $f_q=0$.

Step 3. Solve the problem (9)-(10) (ELP).

Step 4. If a solution is found then go to *Step 5*, otherwise set $n^q=t-1$ and go to *Step 6*.

Step 5. If $F_q(u^{q*}, \phi^{q*}) > f_q$ then set $f_q = F_q(u^{q*}, \phi^{q*})$, $\hat{u}^q = u^{q*}$, $t=t+1$ and go to *Step 3*, otherwise set $n^q=t-1$ go to *Step 6*.

Step 6. If $q<N$ then set $q=q+1$ and go to *Step 2*, otherwise go to *Step 7*.

Step 7. Set $n=\sum_{q=1}^{N} n_q$ and form the vector $u^*=(\hat{u}^1,\ldots,\hat{u}^n)$ that corresponds to the local maximum point of the problem (5)-(6). Find $F(u^*, \phi^*)=\sum_{q=1}^{N} f_q$.

5.2 *Solution strategy for ELP*

Our solution strategy for ELP consists of three major stages:

Stage 1. Generate a number of feasible starting points of the problem (9)-(10), using the algorithm described in Subsection 5.2.1.

Stage 2. Search for the local maximum of the problem (9)-(10) starting from each point obtained at *Stage 1*, using the algorithm described in Subsection 5.2.2.

Stage 3. Choose the best local maximum from those found at *Stage 2*.

For the sake of simplicity we further omit the index q for a convex polygon in the problem (9)-(10).

5.2.1 Starting feasible parameters algorithm (SFP)

Now we describe the algorithm for generating feasible starting points of the problem (9)-(10). Let a convex polygon $\mathbf{P}$ be given by its vertices $p_s=(x_s^p, y_s^p)$, $s \in I_m$.

Step 1. Within $\mathbf{P}$, generate a set of n randomly chosen centers $v_i^0=(x_i^0, y_i^0)$ of ellipses E_i, $i \in I_n$, using the formula

$$v_i^0 = \sum_{s=1}^{m} \alpha_{is} p_s, \ \sum_{s=1}^{m} \alpha_{is} = 1, 0 \le \alpha_{is} \le 1, s \in I_m.$$

To find $\alpha_{is}, s \in I_m$ we randomly generate m positive numbers $n_{is}, s \in I_m$, and derive $\alpha_{is} = \dfrac{n_{is}}{\sum_{s=1}^{m} n_{is}}, s \in I_m.$

Step 2. Form a set of circles $C_i, i \in I_n$, of a variable radius $\lambda b'$ and centers $v_i^0, i \in I_n$, where λ is a variable homothetic coefficient (scaling parameter).

Step 3. Solve the following optimization subproblem, starting from the point $(v^0 = (v_1^0, \ldots, v_n^0), \ \lambda^0 = 0)$:

$$\lambda^* = \max_{(v,\lambda) \in V \subset R^{2n+1}} \lambda,$$

$$V = \{(v,\lambda) \in R^{2n+1} : \Phi^{C_i C_j}(v_i, v_j, \lambda) \ge 0, (i,j) \in \Xi, \Phi^{C_i \mathbf{P}^*}(v_i, \lambda) \ge 0, i \in I_n, 0 \le \lambda \le 1\},$$

where

$$v = (v_1, v_2, \ldots, v_n), \ v_i = (x_i, y_i),$$

$$\Phi^{C_i C_j}(v_i, v_j, \lambda) = (x_i - x_j)^2 + (y_i - y_j)^2 - \lambda^2 \cdot (2b' + \rho)^2,$$

is the normalized *phi*-function for the two circles C_i and C_j of a variable radius $\lambda b'$,

$$\Phi^{C_i \mathbf{P}^*}(v_i, \lambda) = \min_{s=1,\ldots,m} (x_i \cdot \cos\phi_s + y_i \cdot \sin\phi_s + \gamma_s - \lambda b'),$$

is the normalized *phi*-function for the circle C_i of a variable radius $\lambda b'$ and object $\mathbf{P}^*$.

If $\lambda^* < 1$ then feasible starting point has not been found and we stop our procedure, otherwise we go to the next step.

Step 4. Generate, randomly, rotation parameters $\theta_i^1 \in [0, \pi)$ of the ellipses $E_i, i \in I_n$.

Step 5. Return the vector $u^1 = (u_1^1, \ldots u_n^1)$, where $u_i^1 = (v_i^1, \theta_i^1, a_i^1 = b', b_i^1 = b')$ as a starting parameters for local optimization algorithm (see subsection below).

For a large number of ellipses, the problem (9)-(10) cannot be solved by direct use of most of NLP-solvers even starting from the feasible point. Therefore we propose an iterative optimization algorithm to search for the local maxima of the problem as a *new modification* of the LOFRT procedure introduced in (Stoyan, Pankratov, and Romanova 2016) for the packing problem of ellipses in a minimum area rectangle.

5.2.2 Local optimization algorithm

Our algorithm reduces the large scale problem (9)-(10) to a sequence of nonlinear programming subproblems of smaller dimension ($O(n)$ variables and nonlinear constraints). The key idea of the algorithm is as follows. For each vector of the feasible placement parameters of the ellipses, we construct fixed rectangular ε-containers ($\varepsilon>0$ is a decomposition step of our algorithm). Then we allow each ellipse to move within the appropriate ε-container. We describe the motion of each ellipse by a system of four ε-inequalities. Then we form a subset of the feasible set W_q in the following way: we add the $O(n)$ ε-inequalities (for all the ellipses) to the constraints (10) and then delete the $O(n^2)$ *phi*-inequalities corresponding to the pairs of ellipses with non- overlapping individual containers. Some redundant containment constraints are also deleted.

While deleting quasi-*phi*-functions for some pairs of ellipses we also delete the corresponding auxiliary variables. This results in reducing the number of variables in the subproblem. Then we search for the local maximum for the subproblem with $O(n)$ variables and nonlinear constraints. This local maximum is then used as a starting point for the next iteration. On the last iteration of the algorithm we find the local maximum of the problem (9)-(10).

Let us consider the algorithm in details. Let u^1 be one of the points found by the SFP algorithm. Now we describe our local optimization algorithm, which is an iterative decomposition procedure. We denote the value of the algorithm decomposition step by ε and assume that $\varepsilon = S/\pi n \cdot b'^2$, where S is the area of the container **P**.

Step 1. Let $k=1$.

Step 2. Construct a fixed rectangular ε-container $\Omega_i^k \supset E_i(u_i^k)$ of sizes $2\cdot a_i+\rho+\varepsilon$ and $2\cdot b_i+\rho+\varepsilon$ with the center point v_i^k for each $i\in I_n$.

Step 3. Create a system of auxiliary inequality constraints of each ellipse E_i, that allow the ellipse to grow and move inside the ε-container Ω_i^k, using the *phi*-function of the ellipse $E_i(u_i)$ and $\Omega_i^{k*} = R^2 \setminus \mathrm{int}\Omega_i^k$ of the form

$$\Phi^{E_i\Omega_i^{k*}}(u_i) = \min\{f_{i1}^k(u_i), f_{i2}^k(u_i), f_{i3}^k(u_i), f_{i4}^k(u_i)\},$$

where

$$f_{i1}^k(u_i) = (x_i - x_i^k)\cdot\cos\theta_i^k + (y_i - y_i^k)\cdot\sin\theta_i^k + \Delta_{i1}^k;\ f_{i2}^k(u_i) = -(x_i - x_i^k)\cdot\cos\theta_i^k - (y_i - y_i^k)\cdot\sin\theta_i^k + \Delta_{i1}^k,$$

$$f_{i3}^k(u_i) = (x_i - x_i^k)\cdot\sin\theta_i^k - (y_i - y_i^k)\cdot\cos\theta_i^k + \Delta_{i3}^k;\ f_{i4}^k(u_i) = -(x_i - x_i^k)\cdot\sin\theta_i^k + (y_i - y_i^k)\cdot\cos\theta_i^k + \Delta_{i3}^k,$$

$$\Delta_{i1}^k = a_i + 0.5(\rho+\varepsilon) - \sqrt{a_i^2\cos^2(\theta_i+\theta_i^k) + b_i^2\sin^2(\theta_i+\theta_i^k)},$$

$$\Delta_{i3}^k = b_i + 0.5(\rho+\varepsilon) - \sqrt{a_i^2 \sin^2(\theta_i + \theta_i^k) + b_i^2 \cos^2(\theta_i + \theta_i^k)}\,.$$

We note that $v^k = (x^k, y^k)$, θ^k are constants. Thus, the inequality $\Phi^{E_i \Omega_i^{k*}}(u_i) \geq 0$ is equivalent to the system of the four inequalities $f_{il}^k(u_i) \geq 0$, $l = 1,\ldots,4$, $i \in I_n$.

Step 4. Construct an index set that involves such pairs (i, j) of the ellipses $E_i(u_i)$ and $E_j(u_j)$ for which the ε-containers Ω_i^k and Ω_j^k overlap each other, i.e.

$$\Xi^k = \{(i, j) : \Phi^{\Omega_i^k \Omega_j^k}(u_i^k, u_j^k) < 0, i < j \in I_n\},$$

where $\Phi^{\Omega_i^k \Omega_j^k}(u_i^k, u_j^k)$ is the *phi*-function for $\Omega_i^k(u_i^k)$ and $\Omega_j^k(u_j^k)$ (Chernov, Stoyan, and Romanova 2010).

If two ε-containers Ω_i^k and Ω_j^k do not have common interior points (i.e. $\Phi^{\Omega_i^k \Omega_j^k}(u_i^k, u_j^k) \geq 0$), then we do not check the non-overlapping constraint for the corresponding pair of the ellipses E_i and E_j.

Step 5. Construct an index set that involves such pairs (i, s) of the ellipse $E_i(u_i)$ and half plane P_s^* for which ε-container Ω_i^k and P_s^* overlap each other, i.e. $\Xi^{*k} = \{(i,s) : \Phi^{\Omega_i^k P_s^*}(u_i^k) < 0, s \in I_m, i \in I_n\}$, where $\Phi^{\Omega_i^k P_s^*}(u_i^k)$ is the *phi*-function for the polygon $\Omega_i^k(u_i^k)$ and half plane P_s^* (Chernov, Stoyan, and Romanova 2010).

In other words, if the ε-container Ω_i^k and half plane P_s^* have common interior points (i.e. $\Phi^{\Omega_i^k P_s^*}(u_i^k) < 0$), then we take into account the containment constraint for the corresponding pair of objects.

Step 6. Construct a vector of starting values for the auxiliary variables $\phi_{w_k}^k = (\phi_{ij}^k, (i, j) \in \Xi_k)$.

For each pair $(i, j) \in (\Xi \setminus \Xi_k)$ we search for the maximum value of the auxiliary variable ϕ_{ij}, using the following non-constrained nonlinear optimization problem:

$$\phi_{ij}^k = \arg \max_{\phi_{ij} \in [0, 2\pi] \subset R^1} \Phi'^{E_i E_j}(u_i^k, u_j^k, \phi_{ij}),$$

where u_i^k, u_j^k are fixed parameters.

Step 7. Solve the k-th subproblem, starting from the feasible point $(u^k, \phi_{w_k}^k) = (x^k, y^k, \theta^k, a^k, b^k, \phi_{w_k}^k)$:

$$\max_{(u^k,\phi^k_{w_k})\in W_k} F(u,\phi),$$

$$W_k = \{(u^k,\phi^k_{w_k}) \in R^{\sigma-\sigma_k} : \Phi'^{E_iE_j}(u_i,u_j,\phi_{ij}) \geq 0, (i,j)\in \Xi_k,$$

$$\Phi^*_{is}(u_i) \geq 0, (i,s)\in \Xi^*_k, \Phi^{E_i\Omega_i^{k*}}(u_i) \geq 0, a_i \geq b_i, b_i \geq b', a_i \leq a', d' \leq \frac{a_i}{b_i} \leq d'', i \in I_n\}.$$

Here $F(u,\phi)=\pi\sum_{i=1}^{n} a_i b_i$, the quasi-*phi*-function $\Phi'^{E_iE_j}(u_i,u_j,\phi_{ij})$ is defined in (4), the *phi*-function $\Phi^*_{is}(u_i)$ is defined by (3), $\Phi^{E_i\Omega_i^{k*}}(u_i)$ is defined in *Step 3*, Ξ_k is defined in *Step 4*, Ξ^*_k is defined in *Step 5*, $\sigma_k = card(\Xi \setminus \Xi^k)$.

Step 8. If $F(u^{k*},\phi^*_{w_k}) - F(u^{k-1*},\phi^*_{w_{k-1}}) \leq 0.0001$ we stop our procedure, otherwise we set $u^{k+1} = u^{k*}$, take $k = k+1$ and go to *Step 2*.

Our algorithm is able to control only $O(n)$ pairs of ellipses, because for each ellipse only its "ε-neighbours" have to be monitored. This algorithm becomes an efficient for $n > 10$.

6. Computational results

6.1 *The algorithm application for additive manufacturing*

The presented algorithm was applied to design a geometry of a part for the so-called support free 3D printing (Gibson, Rosen, and Stucker 2015). This geometry is the result of solution to topological optimization problem (Gibson, Rosen, and Stucker 2015) for a 100 mm×40 mm×2 mm plane part, which is rigidly fixed at its end and loaded in the lower part of the opposite side with the load P (Fig. 3,a). One of the benchmark solutions of the problem is the part investigated in (Gibson, Rosen, and Stucker 2015) with its frontal projection shown in Fig. 3,b. Note that this design scheme is quite common when testing new topological optimization algorithms (see, e.g., (Jain and Saxena 2010)).

Direct 3D printing of the given part (Fig. 3,b), using, in particular, the DMLS technology (Manfredi et al. 2013), leads to unexpected printing results (Gibson, Rosen, and Stucker 2015). To exclude such cases (including the case when part fragments not adjoining the work platform lower layers are printed) the dedicated programs used for preparing models for 3D printing provide for generating so-called supports. These supports, thin-wall stays, considered as auxiliary elements to be removed after printing has been completed. As an example, Fig. 3,c shows the topology of an optimized 3D part prepared for printing using specialized software. Besides, supports printed using the DMLS technology are often fused to the part walls. Hence, these supports can be removed completely and with quality exclusively by using machining

units with dedicated tooling.

The aforesaid determines the topicality of the publications on developing a method for designing support-free models (the lightweight and support free (L&S) design method) for their subsequent printing, including the use of the DMLS technology. Thereat, the auxiliary (supporting) elements generated using this method, in contrast to supports in the classical sense, are not removed after the part printing has been completed. This cuts production costs and runtime. For the part being investigated, at the initial $\alpha = 45°$ (angle of inclination of supporting elements) and $d = 1$ mm (their thickness), the authors of (Gibson, Rosen, and Stucker 2015) have obtained the model whose topology is shown in Fig. 3,d.

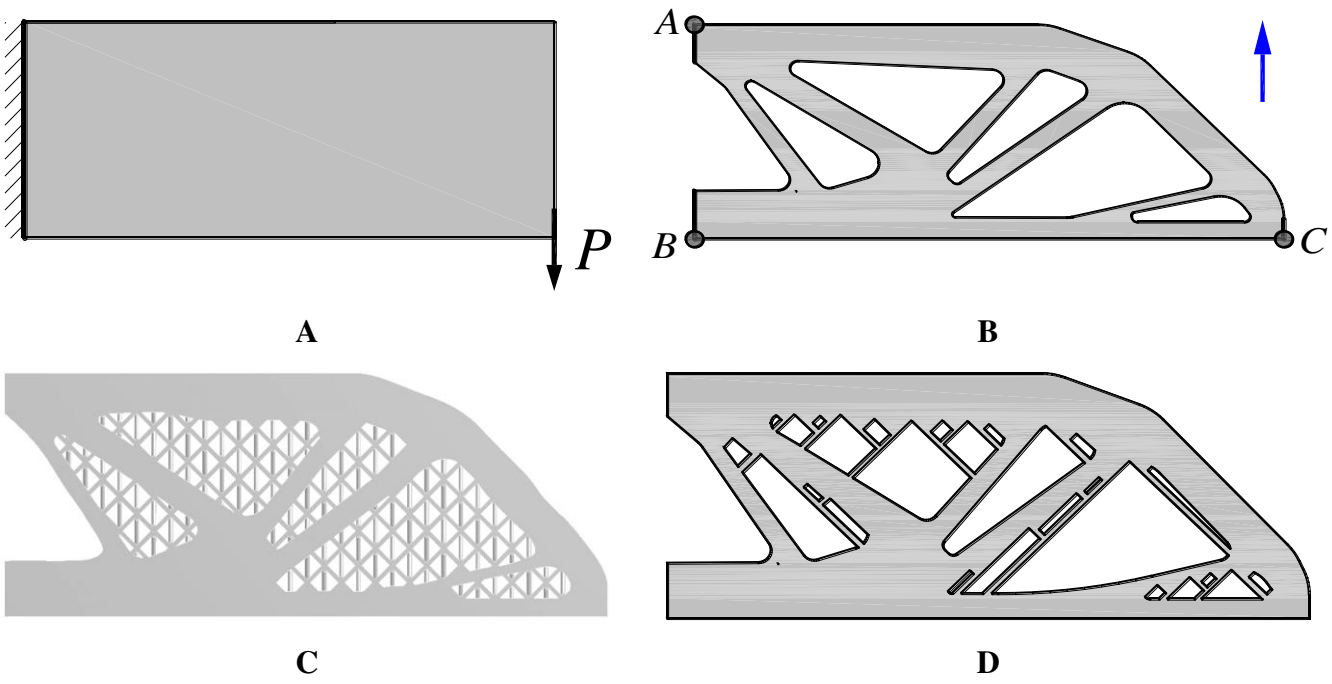

Fig. 3 – The part under investigation

Moreover, the part generated using the L&S method (Fig. 3,d) has sharp changes in the shape of its outer surface in the form of inner corners. They represent the so-called stress concentrators that cause local increases in mechanical stress. This is demonstrated by the results of computing the stress state influenced by a static load $P = 100$ N (Fig. 4). The load scheme is similar to that in Fig. 3,a. If one does not account for the pattern of the stress-strain state in the part fastening zones and load application points (A, B and C, Fig 3,b), which are equalized owing to different design solutions, the maximum stress in the part itself is 40 MPa (Fig. 4,a). A comparable stress value was also obtained for the geometry in Fig. 3,c (29.8 MPa, Fig. 4,b). It also occurs in one of the surface sharp inner corner. For comparison, the maximum design stress in the initial geometry (Fig. 3,b) for an identical computation scheme is virtually twice less – 20.5 MPa (Fig. 4,c). The zones of occurrence of the maximum stress in the areas of the parts under investigation are designated by dark circles in Fig. 4.

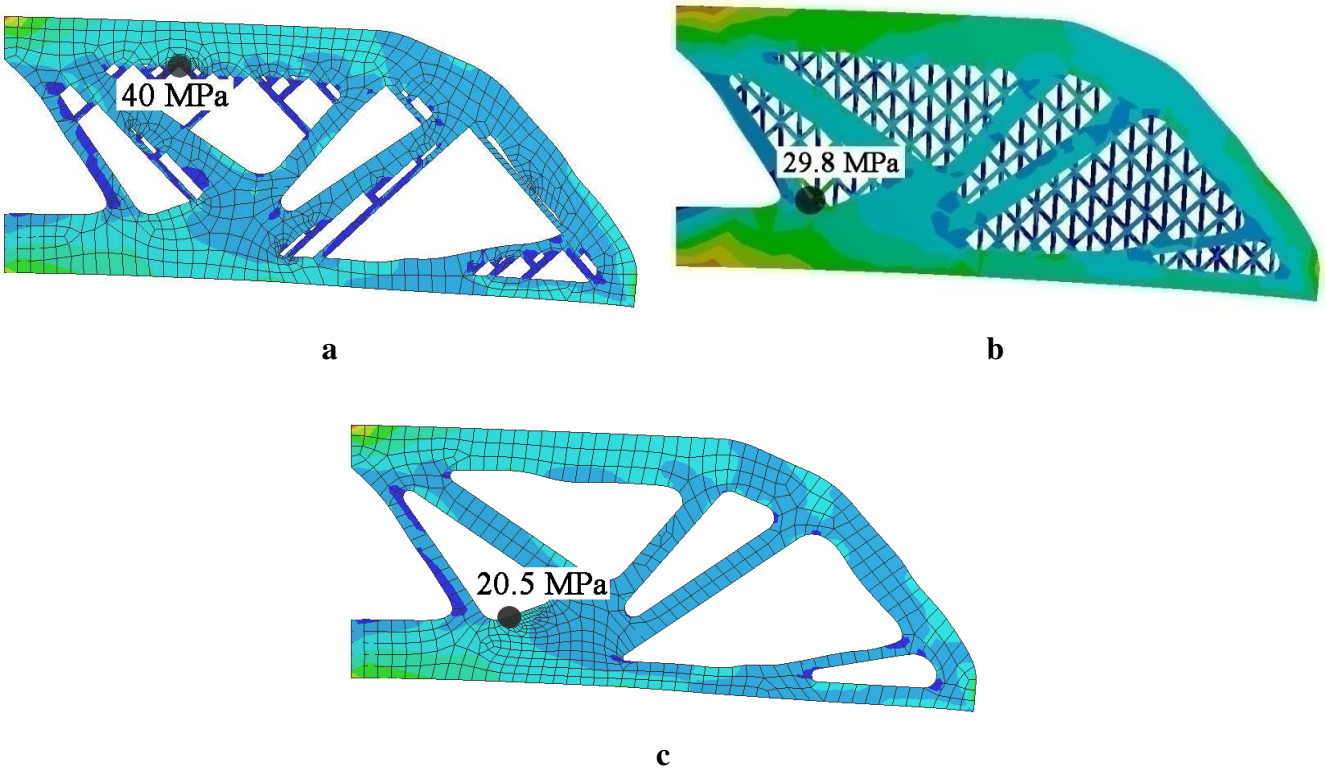

Fig. 4 – Stress state of the part

It should be noted that the computations were performed using a dedicated software complex realizing the FEM. The solution accuracy and convergence were controlled both by using the second-order finite elements and decreasing the grid size near the concentrators. Supposed that the parts were made of the AlSi10Mg powder material using the DMLS technology (the print direction coincides with the arrow in Fig. 3,b). Based on analyzing data (Leary et al. 2016, Manfredi et al. 2013; Brandl et al. 2012; Kempen et al. 2012) on the AlSi10Mg properties the following values are taken: density ρ =2670 kg/m3; elasticity modulus $E_x = E_y$ =70 GPa, E_z =60 GPa; Poisson coefficient ν =0.33; proportional elastic limit σ_Y =240 MPa; yield value σ_U =345 MPa.

An alternative geometry both without stress concentrators in the form of inner sharp corners and adapted for direct printing using the DMLS technology can be built with the help of the algorithm described in the Section 5. In this case we have area Ω which involves five disjoint convex polygons $\mathbf{P}_q$ (see Fig. 3,b), i.e. $N = 5$, $\Omega = \bigcup_{q=1}^{N} \mathbf{P}_q$. Each polygon (denoted with Roman numerals I–V) is given by the coordinates of its vertices in the fixed coordinate system O*xy* (Fig. 5).

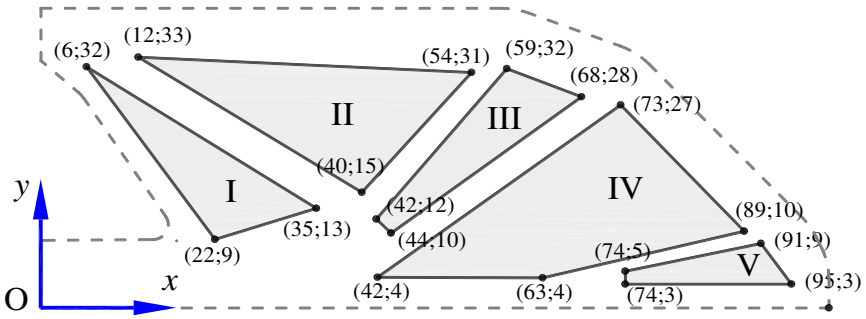

Fig. 5 – The polygonal disconnected domain Ω that involves five convex components

The solution of the ellipses layout problem is shown in Fig. 6,a. The following design parameters are taken: $a \le a' = 7$, $b \ge b' = 1$, $1 \le \frac{a_i}{b_i} \le 3$. The minimum distance between the ellipses (the minimum wall thickness) is assumed to be $\rho = 0.4$. The solution is a collection of $n^* = 18$ ellipses. Dimensions and placement parameters of the ellipses are provided in Appendix A.

It is obvious that the described algorithm is also applicable for solving the circular layout problem – it is sufficient to set the parameters a and b, a' and b' to be equal to each other. The result of implementing the developed algorithm with $a' = b' = r^* = 7$ is presented in Fig. 6.b (the minimum allowable distance, as before, is equal to $\rho = 0.4$). The number of circles is $n^* = 22$. Radii and placement parameters of the circles are provided in Appendix A.

The total area occupied by the elliptical holes in the disconnected area Ω is $F(u^*) = \sum_{q=1}^{N} F_q(u^{q*}) = 882.1334$ ($\{F_q(u^{q*}); q = 1,\ldots,5\} = \{123.4180,\ 237.6701,\ 117.1534,\ 348.6663,\ 55.2254\}$) as presented in Fig. 6a. Computational time is 811.798 sec. To solve the problem with circles we spent more computational time (1325.74 sec), while the total area $F(u^*)$ is slightly less, 829.1148 ($\{F_q(u^{q*}); q = 1,\ldots,5\} = \{112.0467,\ 231.3580,\ 101.8417,\ 339.9569,\ 43.9114\}$) as presented in Fig. 6b. Since the total area of elliptic holes (882.1334) is larger than the area of circular holes (829.1148), the part presented in Fig. 6b determines a bigger mass comparing with the part presented in Fig. 6a, namely: **13.05** grams vs **12.8** grams.

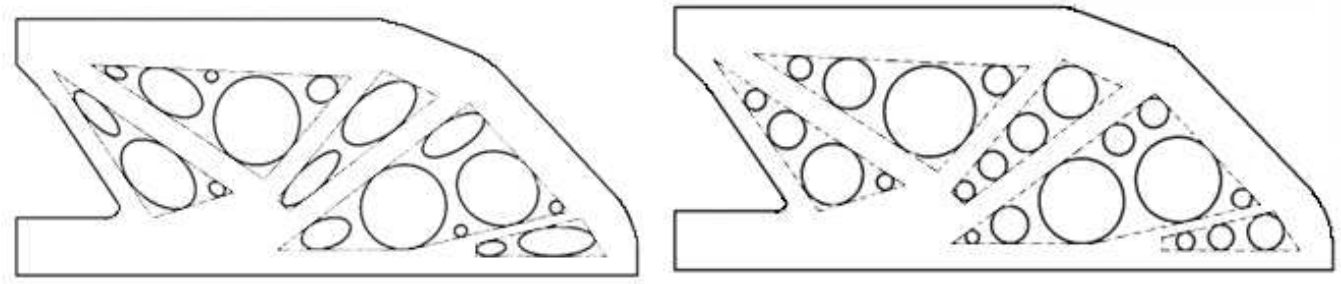

a **b**

Fig. 6 – Frontal surface of the part using computational results:
a) with elliptical holes; b) with round holes

The result of the subsequent finite-element analysis of the stressed state of the obtained parts is presented in Fig. 7 (the computational scheme is similar to that described above).

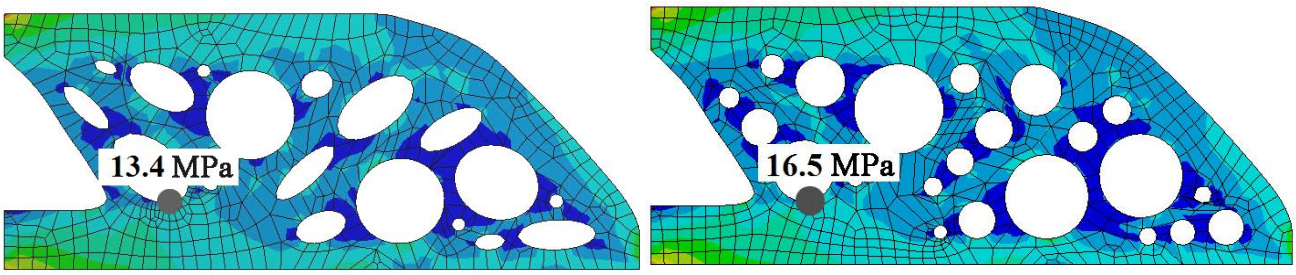

a **b**

Fig. 7 – Mechanical stress of the parts:
a) with elliptical holes; b) with round holes

In these cases the average level of mechanical stress is much smaller than that in the previous models and the maximum mechanical stresses in the investigated zone do not exceed **13.4** MPa for the part with **elliptical** holes and **16.5** MPa in the case of circular holes. This is due to both the absence of geometric stress concentrators and a slightly larger mass of the part. In particular, the mass of the part in Fig. 3,b is **10.7 grams**; in Fig. 3,c and 3,d – **11.9 grams**, whereas the mass of the initial part (Fig. 3,a) is **21.2 grams**. Obviously, increasing the part mass means increasing its production cost and is the cause of growing inertial loads in case of non-stationary vibrations and so forth. However, at the same time, the suggested algorithm for preparing parts' geometry for direct 3D printing, in contrast to the one described in (Gibson, Rosen, and Stucker 2015), is not so sensitive to the printing direction. Fig. 8, in particular, shows the results of 3D printing of the part with elliptical cavities (Fig. 6,a) for its two different orientations on a printer working platform.

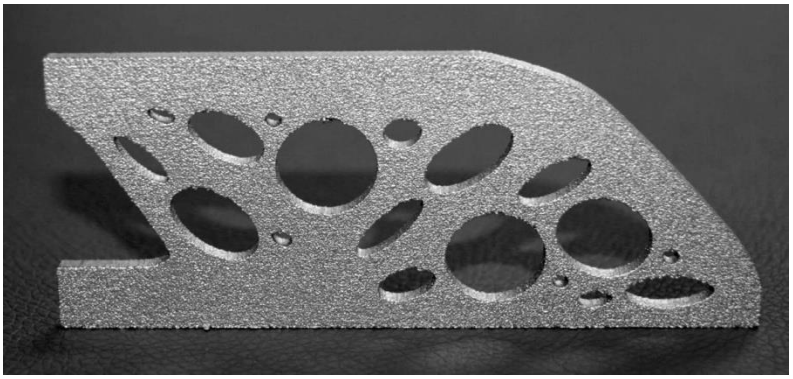

a

b

Fig. 8 – Result of 3D printing
with different orientation of the part

As can be seen from the figure, the finished part, which was obtained using the EOS m270 printer (http://www.eos.info), has no visible defects in both directions of its manufacturing and the geometry of the part practically does not differ from that of the 3D model. Here it should be noted that changing the print direction can be used in case of enhanced requirements to part strength because its material obtained with the DMLS technology, in particular, AlSi10Mg, belongs to the class of transversely isotropic ($E_x = E_y \neq E_z$) ones – by choosing the print direction, the stress state pattern can be slightly "adjusted" for the given static external load.

Thus, the presented ellipses layout algorithm allows obtaining an alternative topology of parts, which is suitable for direct printing using DMLS technology, do not contain stress concentrators and do not sensitive to the printing direction. The presence of surfaces of the simplest form allows reducing surface roughness at the final stage of manufacturing thus affecting the fatigue strength of a part.

6.2 *The algorithm application for packing ellipses into a convex polygonal container*

We also test presented algorithm for the problem (9)-(10) assuming $q = 1$.

Let $\mathbf{P}$ be a convex m-polygon ($m = 9$), given by its vertices (see Appendix A).

We assume that each ellipse has variable semi-axes $a_i \le a'$, $b_i \ge b' = 1$, $1 \le \frac{a_i}{b_i} \le 3$. The minimum allowable distance between each pair of ellipses is $\rho = 0.2$.

In case $a' = 2$ the result of searching for the local maximum is as follows: the number of ellipses is $n^* = 33$, their total area is $F(u^*) =$ 310.5722. Dimensions and placement parameters of the ellipses are

provided in Appendix A. Computational time is 9044.688 sec. The local optimal packing is shown in Fig.9,a.

For $a'=3$ the solution is: the number of ellipses is $n^*=17$, their total area is $F(u^*)=319.7317$. Dimensions and placement parameters of the ellipses are provided in Appendix A. Computational time is 2622.377sec. The result is shown in Fig. 9,b.

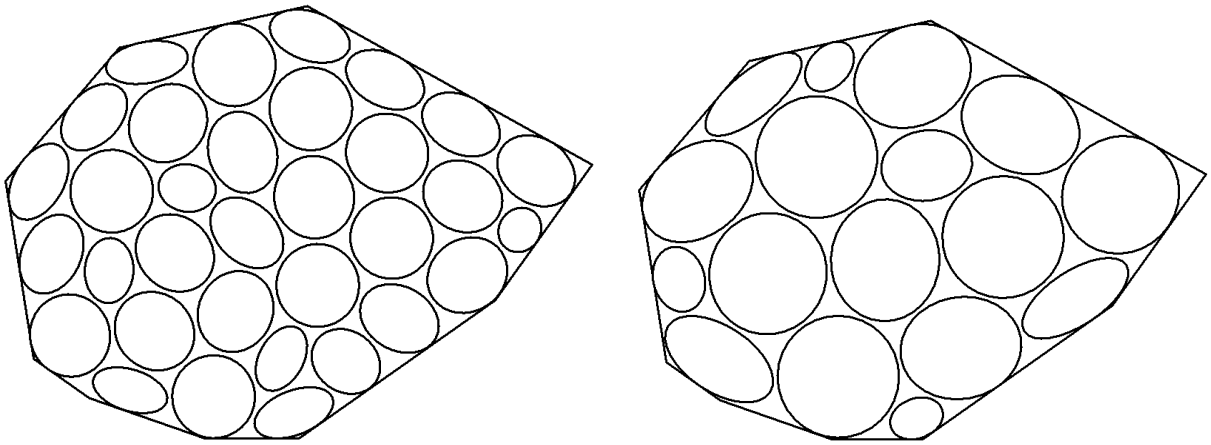

a **b**

Fig. 9 – The local optimal packing: a) $a'=2$; b) $a'=3$

For both cases we used 100 runs of our program (computer – AMD FX™-6100, CPU 3.30 GHz; Programming Language C++; OS Windows 7). For the local optimization we use the IPOPT code (https://projects.coin-or.org/Ipopt).

The results of the computational experiments demonstrate that the main algorithm combined with the reduction technique presented in Section 5.5.2 can manage a large number of ellipses in various convex polygons. Moreover, for the first time the ellipse packing problem was considered for the case when, in addition to continuous translations and rotations, the number of ellipses and their sizes are not fixed and have to be obtained. Also, the minimal allowable distance between ellipses is taking into account. The proposed approach can be naturally generalized for the 3D case.

Acknowledgment

The work of Litvinchev I. was partially supported by CONACYT (Mexico) through the grants #167019 and #293403.

7. Conclusions

A new optimization layout problem for ellipses is considered in the study. Our container is an arbitrary disconnected polygonal area. In the problem the number of ellipses, sizes and placement parameters

of ellipses are variable and have to be defined. Our ellipses can be continuously translated and rotated. Restrictions on the dimensions of ellipses are taken into account. Our objective is to maximize the packing factor. This problem has applications in additive manufacturing, in particular, in part topology preparation for direct support-free production. To state the distance and containment constraints new normalized *phi*-functions and quasi-*phi*-functions are constructed. Our approach results in formulating the layout problem in the form of a nonlinear mathematical programming problem. We develop a new algorithm for constructing feasible starting points and also an optimization procedure to reduce the computational cost of the ellipse packing problem. The case study (optimized topology of the part) solved by the proposed technique indicates that the resulting geometry of the part is not sensitive to the direction of additive manufacturing and does not require so-called supports. Moreover, the maximum mechanical stresses calculated by FEM are slightly lower than those for the original and alternative geometries. In addition, the part surface system itself is simple from the point of view of possible subsequent technological processing, which is especially important for parts under dynamic loads.

The main objective of introducing elliptic cavity system in 3D printing is reducing the weight of the part without losing its mechanical properties. Comparing with circular holes elliptic cavity system is more flexible, i.e. it can be adjusted to the shape of the polygonal domain thus providing more weight savings. From mathematical point of view an ellipse can be considered as a circle defined in a certain non-symmetrical 2-norm (Euclidian norm). Using p-norms ($p \geq 3$) instead of Euclidian norm the so-called ovals or circular-like objects (Litvinchev, Infante, and Ozuna 2015a, Litvinchev, Infante, and Ozuna 2015b) can be used in the cavity system providing tighter approximations of polygons. An interesting direction for the future research is considering different and non-uniform shapes for the cavity system. Moreover, the shapes of the holes can be also be optimized considering. It is also interesting to generalize the proposed models and solution techniques for a 3D cavity system in a 3D part. Some results in this directions are on the way.

References

Araújo Luiz, J.P., Özcan, E., Atkin Jason, A.D., Baumers, M. 2018. "Analysis of irregular three-dimensional packing problems in additive manufacturing: a new taxonomy and dataset." *International Journal of Production Research*. 5920-5934. doi.org/10.1080/00207543.2018.1534016.

Birgin, E.G., Lobato, R.D., Martinez, J.M. 2016. "Packing ellipsoids by nonlinear optimization." *Journal of Global Optimization*. 65(4): 709–743.

Brandl, E., Heckenberger, U., Holzinger, V., Buchbinder, D. 2012. "Additive manufactured AlSi10Mg samples using Selective Laser Melting (SLM): Microstructure, high cycle fatigue, and fracture behavior." *Materials and Design*. 34: 159–169.

Chernov, N., Stoyan, Y., Romanova, T. 2010. "Mathematical model and efficient algorithms for object packing problem." *Computational Geometry: Theory and Applications*, 43(9): 535–553.

Emmendorfer, Leonardo R., Oro, Neuza T., Beckel, Cassia C. (2015). "An application of Hooke and Jeeves Method as a Constructive Heuristic for the Ellipse Packing Problem." *Int. J. Eng. Math. Model*., 2(4): 110–122.

Fasano, G. A. 2015. “Modeling-Based Approach for Non-standard Packing Problems.” In: Fasano,G., Pintér, J.D. (eds.) Optimized Packings and their Applications. Springer Optimization and its Applications. Springer, New York.

Gibson, I., Rosen, D., Stucker, B. 2015. “Additive manufacturing technologies, 3D printing, rapid prototyping, and direct digital manufacturing.” New-York: Springer Science + Business Media.

Huang, X., Xie, Y.M. 2010. “Evolutionary topology optimization of continuum structures: methods and applications.” UK, A John Wiley & Sons Ltd.

Jain, Ch., Saxena, A. 2010. “An improved material-mask overlay strategy for topology optimization of structures and compliant mechanisms.” *Journal of Mechanical Design*. 132(6): 061006-1– 061006-10.

Kallrath, J., Rebennack, S. 2014. “Cutting ellipses from area-minimizing rectangles.” *Journal of Global Optimization*, 59(2): 405–437.

Kampas, F.J., Castillo, I., Pintér, J.D. 2019. “Optimized ellipse packings in regular polygons.” *Optimization Letters*. 75(2): 495–522. doi.org/10.1007/s11590-019-01423-y

Kempen, K., Thijs, L., Humbeeck, J., Kruth, J.-P. 2012. “Mechanical properties of AlSi10Mg produced by Selective Laser Melting.” *Physics Procedia*. 39: 439–446.

Lachmayer, R., Lippert, R. B. 2017. “Additive Manufacturing. Quantifiziert – Visionäre Anwendungen und Stand der Technik.” Berlin: Springer Vieweg Verlag.

Leao Aline, A.S., Toledo Franklina, M.B., Oliveira, J.F., Carravilla, M.A., Alvarez-Valdés, R. 2019. “Irregular packing problems: a review of mathematical models.” *European Journal of Operational Research*. doi.org/10.1016/j.ejor.2019.04.045

Leary, M., Mazur, M., Elambasseril, J., McMillan, M., Chirent, Th., Sun, Y., Qian, M., Easton, M., Brandt, M. 2016. “Selective laser melting (SLM) of AlSi12Mg lattice structures.” *Materials and Design*. 98: 344–357.

Litvinchev, I., Infante, L., Ozuna, L. 2015. “Packing circular-like objects in a rectangular container.” *Journal of Computer and Systems Sciences International*, 54: 259–267.

Litvinchev, I., Infante, L., Ozuna, L. 2015. Approximate packing: integer programming models, valid inequalities and nesting. In: Fasano G., Pinter J.D, (Eds.), Optimized Packings and Their Applications (Ser.: Springer Optimization and Its Applications), 105: 117–135

Liu, J., Ma, Y. 2016. “A survey of manufacturing oriented topology optimization methods.” *Advances in Engineering Software*, 100: 161–175.

Liu, K., Tovar, A. 2014. “An efficient 3D topology optimization code written in MatLab.” *Structural and Multidisciplinary Optimization*, 50: 1175–1196.

Manfredi, D., Calignano, F., Ambrosio, E. P., Krishnan, M. , Canali, R., Biamino, S., Pavese, M., Atzeni, E., Luliano, L., Fino, P., Badini, C. 2013. “Direct Metal Laser Sintering: An additive manufacturing technology ready to produce lightweight structural parts for robotic applications.” *La Metallurgia Italiana,* 105(10): 15–24.

Mokwon Lee, Qing Fang, Youngsong Cho, Joonghyun Ryu, Ligang Liu, Deok-Soo Kim. 2018. “Support-free hollowing for 3D printing via Voronoi diagram of ellipses.” *Computer-Aided Design*, 101: 23–36.

Pankratov, A., Romanova, T., Litvinchev, I. 2018. “Packing ellipses in an optimized rectangular container.” Wireless Networks. doi: 10.1007/s11276-018-1890-1.

Pankratov, A., Romanova, T., Litvinchev, I. 2019. “Packing ellipses in an optimized convex polygon.” *Journal of Global Optimization*, 75(2): 495–522. doi.org/10.1007/s10898-019-00777-y

Romanova, T., Bennell, J., Stoyan, Y., Pankratov, A. 2018. “Packing of concave polyhedra with continuous rotations using nonlinear optimization.” *European Journal of Operational Research*, 268: 37–53.

Stoyan, Y., Pankratov, A., Romanova, T. 2016. “Quasi phi-functions and optimal packing of ellipses.” *Journal of Global Optimization*, 65 (2): 283–307.

Stoyan, Yu., Pankratov, A., Romanova, T. 2015. “Cutting and Packing problems for irregular objects with continuous rotations: mathematical modeling and nonlinear optimization.” *Journal of the Operational Research Society*, 67(5): 786–800.

Stoyan, Yu., Pankratov, A., Romanova, T., Chugay, A. 2015. “Optimized object packings using quasi-phi-functions.” Chapter in contributed book “Optimized Packings and Their Applications”, Editors/ G. Fasano and J.Pintér/ Springer Optimization and its Applications. – New York, 105: 265–291.

Stoyan, Yu., Romanova, T. 2013. “Mathematical models of placement optimisation: two- and three-dimensional problems and applications.” Chapter in contributed book “Modeling and Optimization in

Space Engineering", Editors/ G. Fasano and J.Pintér/ Springer Optimization and its Applications. New York, 73: 363–388.

Appendix A. Data to Section 6

Output data to Subsection 6.1.

The following dimensions of $n^* = 18$ ellipses were obtained by our algorithm:

$\{(a_i^*, b_i^*), i = 1,2,\ldots,n^*\}$ = {(1.451003 1.056384), (4.802429 1.610994), (7.0 4.287956), (7.0 7.0), (1.090857 1.0), (2.595877 2.155090), (1.885885 1.0), (5.641415 3.205164), (7.03.617268), (6.056729 1.976352), (5.562663 2.428522), (6.745289 5.740417), (4.128611 2.363029), (1.115792 1.097139), (1.057427 1.0), (7.0 6.673785), (6.170471 2.357579), (2.435725 1.244570)}.

The following radii of $n^* = 22$ circles were obtained by our algorithm:

$\{r_i^*, i = 1,2,\ldots,n^*\}$ = {1.664237 1.322005 4.758209 2.916789 2.350569 1.905463 7.0 3.935426 1.519199 4.017607 3.013604 2.210498 2.388148 2.292906 1.520114 6.519394 6.534865 2.935743 1.055787 1.399771 2.813647 2.025208}.

Input and output data to Subsection 6.2.

The vertices of the convex m-polygon **P** are given as follows:

$\{(x_s, y_s), s = 1,\ldots,9\}$ = {(-7.2662, 1.5934), (-5.9413, -6.8803), (-3.2915, -8.7339), (2.3109, -10.6632), (6.7020, -10.6632), (16.0520, -4.0809), (20.6702, 2.3878), (7.1184, 9.9159), (-1.8530, 7.9487)}.

The following dimensions of $n^* = 33$ ellipses for $a' = 2$ were obtained by our algorithm:

$\{(a_i^*, b_i^*), i = 1,2,\ldots,n^*\}$ = {(1.7492 1.4524), (2.0 1.0), (2.0 1.7418), (2.0 2.0), (2.0 1.7786), (1.9474 1.6626), (1.1023 1.0), (2.0 1.2051), (2.0 1.0744), (2.0 2.0), (2.0 1.9313), (2.0 2.0), (1.8739 1.2569), (1.6781 1.0738), (2.0 1.4385), (2.0 1.8120), (2.0 1.5823), (2.0 1.6281), (2.0 1.2863), (2.0 1.8644), (2.0 2.0), (1.5703 1.1711), (2.0 2.0), (1.8292 1.0), (1.9948 1.7930), (2.0 1.5395), (2.0 1.3957), (2.0 1.1812), (2.0 1.9569), (2.0 1.4263), (1.4049 1.1291), (2.0 1.7457), (2.0 1.9053) }.

The following dimensions of $n^* = 17$ ellipses for $a' = 3$ were obtained by our algorithm:

$\{(a_i^*, b_i^*), i = 1,2,\ldots,n^*\}$ = {(3.0 2.3386), (3.0 3.0), (2.9681 2.8343), (3.0 2.1999), (1.4309 1.0), (3.0 2.6943), (3.0 2.4986), (3.0 3.0), (2.9251 1.1559), (3.0 1.3474), (2.2677 1.7577), (3.0 2.8846), (1.6366 1.2712), (1.3556 1.0), (3.0 1.6418), (3.0 2.4366) (3.0 3.0)}.